Scientific Research Publishing

Open Journal of Applied Sciences, 2024, 14, 1823-1842
https://www.scirp.org/journal/ojapps
ISSN Online: 2165-3925
ISSN Print: 2165-3917

# Nonlinear Pushover Analysis of the Influences on RC Footing for the External Elevator Well

**Mo Shi[1*], Xiaoyan Xu[2], Yeol Choi[1]**

[1]School of Architecture, Kyungpook National University, Daegu, Republic of Korea
[2]HaXell Elevator Co., Ltd., Shanghai, China
Email: *shimo0204@outlook.jp

**How to cite this paper:** Shi, M., Xu, X.Y. and Choi, Y. (2024) Nonlinear Pushover Analysis of the Influences on RC Footing for the External Elevator Well. *Open Journal of Applied Sciences*, **14**, 1823-1842.
https://doi.org/10.4236/ojapps.2024.147119

**Received:** June 16, 2024
**Accepted:** July 21, 2024
**Published:** July 24, 2024



## Abstract

In contemporary society, reducing carbon dioxide emissions and achieving sustainable development are paramount goals. One effective approach is to preserve existing RC (Reinforced Concrete) buildings rather than demolishing them for new construction. However, a significant challenge arises from the lack of elevator designs in many of these existing RC buildings. Adding an external elevator becomes crucial to solving accessibility issues, enhancing property value, and satisfying modern residential buildings using convenient requirements. However, the structural performance of external elevator wells remains understudied. This research is designed by the actual external elevator project into existing RC buildings in Jinzhong Rd, Shanghai City. Specifically, this research examines five different external elevator wells under nonlinear pushover analysis, each varying in the height of the RC (Reinforced Concrete) footing. By analyzing plastic hinge states, performance points, capacity curves, spectrum curves, layer displacement, and drift ratio, this research aims to provide a comprehensive understanding of how these structures of the external elevator well respond to seismic events. The findings are expected to serve as a valuable reference for future external elevator projects, ensuring the external elevator designs meet the seismic requirements. By emphasizing seismic resistance in the design phase, the research aims to enhance the overall safety and longevity of external elevator systems integrated into existing RC buildings.

## Keywords

Nonlinear Pushover Analysis, External Elevator, Existing RC Buildings, RC Footing, Sustainable Development

## 1. Introduction

Over the past decades, numerous RC frame buildings have been constructed for residential and commercial purposes. Many of these buildings, particularly those built in the 1970s and 1980s, were designed without elevators. In contemporary society, the convenience of building usage has become a priority, making elevator design an essential feature of modern buildings. Reconstructing RC buildings leads to significant environmental damage, highlighting the importance of retrofitting existing structures.

Green retrofitting initiatives play a crucial role in reducing global energy consumption and greenhouse gas emissions, particularly within residential buildings. A substantial body of research has focused on this topic [1]-[5]. For instance, the research of Yongtao Tan *et al.* [1] on revitalizing old residential buildings in Hong Kong, China and the research of Sui Pheng Low *et al.* [2] on enhancing building sustainability in Singapore emphasize the critical role of external elevators. These studies consistently underscore the importance of integrating external elevators into retrofitting projects to meet contemporary environmental and societal standards. Furthermore, to address the issue of elevator traffic efficiency, the research of Mo Shi *et al.* [3] underscores the importance of utilizing advanced technologies. Specifically, the research focuses on the LSTM (Long Short-Term Memory) neural network, a type of recurrent neural network well-suited for time series analysis. By implementing the LSTM neural network, the research aims to analyze and predict elevator traffic patterns accurately. This approach allows for more efficient management of elevator systems, optimizing performance and reducing wait times for users. The research of Mo Shi *et al.* [3] demonstrates how integrating modern machine-learning techniques can significantly enhance the operational efficiency of elevator systems.

Although there has been significant research on incorporating external elevators into existing RC buildings and numerous advantages have been identified, a notable gap remains in addressing seismic concerns. As many previous researches point out [6]-[8], earthquakes pose a longstanding challenge, especially in regions susceptible to seismic activity, where maintaining structural integrity is crucial for minimizing damage and ensuring public safety. Given that the external elevator shaft becomes a critical structural element in existing RC buildings, it is essential to assess the structural implications of installing external elevators, particularly their potential vulnerability to seismic forces.

In the field of structural engineering, pushover analysis is a prominent nonlinear static analysis technique used to assess the seismic performance of buildings [9]-[15]. As M. Bhandari *et al.* [16] emphasize, this method illustrates how a structure behaves when subjected to seismic loading by applying progressive lateral forces that mimic the effects of an earthquake. Referring to the research of Mohammed Ismaeil *et al.* [17], four typical existing RC buildings in Sudan were investigated to assess the structural performance under seismic events. This research employed nonlinear pushover analysis as outlined in the ATC-40 guide-

lines. By applying this method, this research indicates the critical need for seismic evaluation of existing buildings, ensuring the satisfaction of the necessary safety standards and the ability to withstand potential seismic activities. Through nonlinear pushover analysis, the structural response and potential weak points and failure modes can be identified, allowing for more effective design and retrofitting strategies to enhance building resilience during seismic events.

In this research, an external elevator project for an existing RC building in Jinzhong Rd, Shanghai City (121˚36'69"E, 31˚21'99"N) is the focal point as **Figure 1** shows. This research involves simulating the specific external elevator well and performing structural analysis using the nonlinear pushover analysis approach. The RC footing can be considered as the foundation of the external elevator well, and it also can be considered as a critical component commonly on the structure of the external elevator well. Therefore, it is essential to examine how different heights of RC footings influence the structural performance of the external elevator well. In this research, five different cases with varying heights of RC footings in the external elevator pit are analyzed to determine the structural influences. In summary, this research is focused on analyzing the influences of varying heights of RC footings on the performance of external elevator wells using nonlinear pushover analysis. By examining different RC footing heights, the study seeks to understand how these variations influence the structural behavior of external elevator wells, especially under seismic conditions. The insights gained from this research are expected to be valuable for future engineering projects involving external elevators in existing RC buildings. These findings aim to enhance the overall structural performance and safety of external elevator wells, ensuring the external elevator wells are better equipped to withstand seismic damage.

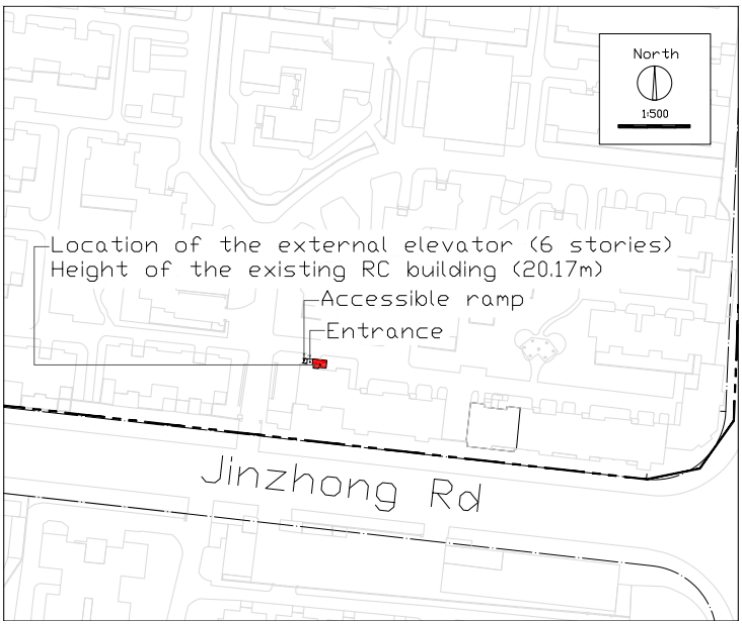


**Figure 1.** Location of the external elevator project.

## 2. Description of the Research

### 2.1. Description of the Structure

For the specific external elevator project in an existing RC building in Shanghai City, the external elevator well is designed as a height of 19.6 m and a width of 2 m, as illustrated in Figure 2. According to Figure 3, the cross-section of the elevator well is square, measuring 2 m × 2 m. The RC pit and footing are both designed with a thickness of 250 mm, while the square steel of the external elevator well is designed as 200 mm × 200 mm.

As illustrated in Figure 2, the design for the external elevator pit has a height of 1.5 m. Based on the same external elevator structural design, five different RC footing cases are designed. These concrete footings are designed at varying heights of 300 mm, 600 mm, 900 mm, 1200 mm, and 1500 mm. This range of designs allows for a comparative analysis of the structural implications at different RC footing heights, ensuring comprehensive findings of the influences on the overall stability and performance of the external elevator well.

For the external elevator project in an existing RC building in Shanghai City, the design specifies that the concrete pit and RC footing are to be 250 mm thick. This dimension is slightly larger than the square steel sections (200 mm × 200 mm) that form the main structural framework of the external elevator well as Figure 3 shows. This design ensures that the concrete components adequately accommodate and support the square steel installations, providing enhanced stability and structural integrity for the external elevator well.

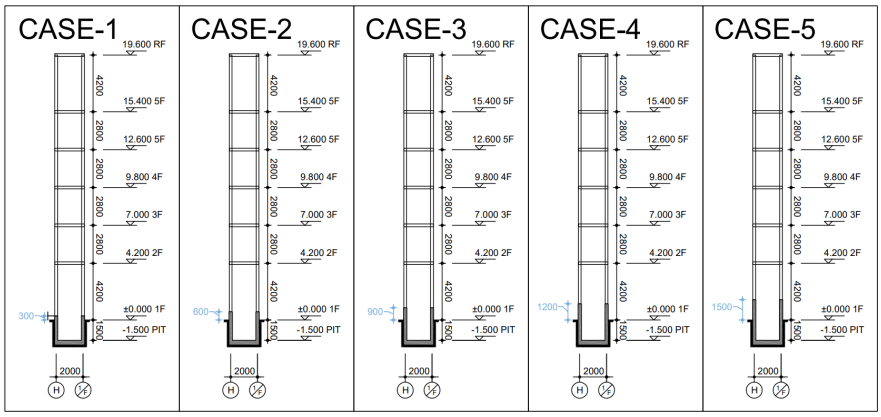


Figure 2. Design of the external elevator well.

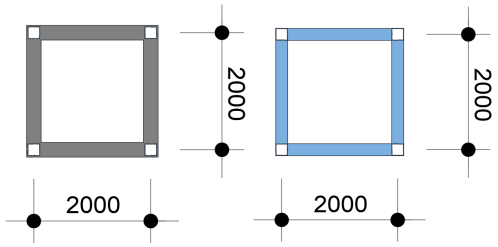


(a) Concrete pit (b) Steel structure

Figure 3. Sections of the external elevator well.

## 2.2. Description of Section and Material

The research of Mohammad T. Alkhamis *et al.* [18] underscores the critical role that cement properties play in affecting the stresses and strains within concrete components. This insight is particularly relevant when selecting materials for the concrete footing of external elevators, where the performance of concrete under seismic load is crucial. Especially, the research of Mohammad T. Alkhamis *et al.* [18] underscores the critical role that cement properties play in affecting the stresses and strains within concrete components.

In this research, the concrete selected is C30, according to the Chinese standards GB 50010-2010 (Code for Design of Concrete Structures) and GB 50011-2010 (Code for Seismic Design of Buildings), as shown in Table 1. The code specifies the concrete compressive strength and the expected concrete compressive strength is 20.1 MPa. The C30 concrete is specifically used in constructing the external elevator pit and the RC footing parts of the project.

According to the Chinese standards GB 50010-2010 (Code for Design of Concrete Structures) and GB 50011-2010 (Code for Seismic Design of Buildings), the rebar selected is HRB400 as illustrated in Table 2. The code specifies that the rebar has a minimum yield stress of 400 MPa and a minimum tensile stress of 540 MPa. The HRB400 rebar is used in conjunction with C30 concrete in constructing the external elevator pit and the RC footing parts.

The design for the external elevator pit and RC footing includes a total section thickness of 250 mm. According to the specific design of the external elevator project, this includes a concrete cover of 36.35 mm. The rebar is arranged in a grid pattern with two layers at 0˚ and 90˚ on both the top and bottom of the section.

**Table 1.** Concrete property.

| | |
|---|---|
| Weight per unit volume | 25,000 N/m$^3$ |
| Mass per unit volume | 2550 kg/m$^3$ |
| Modulus of Elasticity (E) | 30,000 MPa |
| Poisson (U) | 0.2 |
| Coefficient of Thermal Expansion (A) | 1.000E−05 |
| Shear Modulus (G) | 12,500 MPa |
| Specified Compressive Strength (Fck) | 20.1 MPa |
| Expected Compressive Strength (Fek) | 20.1 MPa |

**Table 2.** Rebar property.

| | |
|---|---|
| Weight per unit volume | 77,000 N/m$^3$ |
| Mass per unit volume | 7850 kg/m$^3$ |
| Modulus of Elasticity (E) | 200,000 MPa |
| Poisson (U) | 0.3 |
| Coefficient of Thermal Expansion (A) | 1.170E−05 |
| Minimum Yield Stress (Fy) | 400 MPa |
| Minimum Tensile Stress (Fu) | 540 MPa |
| Expected Yield Stress (Fye) | 440 MPa |
| Expected Tensile Stress (Fue) | 590 MPa |

The primary structure of the external elevator well, as depicted in Figure 4, is constructed using square steel. The section of the square steel measures 200 mm × 200 mm, with a thickness of 8 mm. The design of the primary structure of the external elevator well is based on the specific requirements of this project, ensuring that the structural framework is both robust and capable of supporting the external elevator system effectively.

For the square steel members used in the external elevator well, the selected steel is Q235, in accordance with Chinese standards GB/T 700-2006 (Carbon Structural Steels) and GB 50011-2010 (Code for Seismic Design of Buildings). As illustrated in Table 3, the code of GB/T 700-2006 specifies that Q235 steel has a minimum yield stress of 235 MPa and a minimum tensile stress of 370 MPa.

In this research, three main materials are utilized for constructing the external elevator well: Q235 square steel, HRB400 rebar, and C30 concrete, and these materials form the structure of the external elevator well. This research incorporates five different design variations of the elevator well, as illustrated in Figure 2. The primary objective of this research is to analyze how the RC footing influences the overall structural integrity and performance of the external elevator well. By examining these different designs, the research aims to provide insights into optimizing the structural components for enhanced stability and durability.

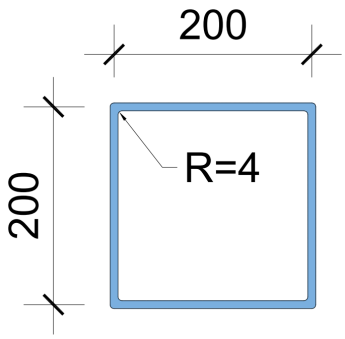


Figure 4. Section of the square steel.

Table 3. Square steel property.

| | |
|---|---|
| Weight per unit volume | 77,000 N/m$^3$ |
| Mass per unit volume | 7850 kg/m$^3$ |
| Modulus of Elasticity (E) | 206,000 MPa |
| Poisson (U) | 0.3 |
| Coefficient of Thermal Expansion (A) | 1.200E−05 |
| Shear Modulus (G) | 79230.77 MPa |
| Minimum Yield Stress (Fy) | 235 MPa |
| Minimum Tensile Stress (Fu) | 370 MPa |
| Expected Yield Stress (Fye) | 260 MPa |
| Expected Tensile Stress (Fue) | 410 MPa |

## 2.3. Description of Load Design

Based on the specific design of the external elevator well for this project and in accordance with GB/T 7588-2020 (Safety Rules for the Construction and Installation of Lifts), the passenger load capacity of the elevator is set at 630 kg. Additionally, using the scale coefficient, the self-weight of the elevator cabin is calculated to be 787.5 kg, as detailed in Table 4.

Table 4. Load design.

| Passenger Load<br>kg | Cabin Load<br>kg | Live Load<br>kN/m | Dead Load<br>kN/m |
|---|---|---|---|
| 630 | 787.5 | 1.54 | 1.93 |

Furthermore, in accordance with the Chinese standard GB 50011-2010 (Code for Seismic Design of Buildings), the Dead Load and Live Load for the structure can be determined using specific equations as below:

$$\omega_D = \frac{P_D}{L} \tag{1}$$

$$\omega_L = \frac{P_L}{L} \tag{2}$$

where $P_D$ is the force from the Dead Load and $\omega_D$ is the uniform load from the Dead Load. On the other hand, $P_L$ is the force from the Live Load and $\omega_L$ is the uniform load from the Live Load. Through the calculation above, the value of Dead Load is given in 1.93 kN/m, and the value of Live Load is given in 1.54 kN/m as Table 4 illustrates.

The calculation is crucial for accurately assessing the loads that the structure will need to support. This ensures that the design meets the required seismic performance criteria, which is vital for the safety and stability of the structure. Additionally, these calculations are integral to the structural analysis conducted in this research, specifically under the pushover analysis method. This analysis helps evaluate how the structure responds to seismic forces, further ensuring its resilience and reliability.

## 2.4. Nonlinear Pushover Analysis

To satisfy the simulation requirements for nonlinear pushover analysis, it is essential to assign plastic hinge properties to each structural component. This involves defining specific characteristics for these plastic hinges to accurately simulate how the components will behave under nonlinear pushover analysis. The criteria for determining these properties are outlined in ASCE 41-13 and this code is endorsed and supported by SAP 2000, ensuring that the analysis is both accurate and consistent with industry practices. These measures are crucial for a thorough and reliable structural analysis.

The plastic hinges for the column section are established by ASCE 41-13 standards. This modeling process specifically follows the parameters and criteria

outlined in Tab. 9-6, which focuses on steel columns in nonlinear procedures. The degree of freedom for the column is set as P-M2-M3, which represents the axial force and moments in two directions. This approach ensures that the modeling accurately reflects the column's behavior under various loads and stresses, providing a reliable basis for the nonlinear analysis.

The beam section of the external elevator structure uses the same square steel as the column section and follows Tab. 9-6 in ASCE 41-13 guidelines for the plastic hinge design, however, unlike the column section, which has a degree of freedom set as P-M2-M3, the degree of freedom is established as M3 for beam section, reflecting the specific characteristics of beam. This differentiation ensures that the plastic hinge modeling accurately represents the behaviors and mechanic responses of both beams and columns within the structural analysis.

Regarding the nonlinear pushover analysis in this research, considering load combinations is a critical aspect that significantly influences the structural assessment. The Chinese standard GB 50011-2010 (Code for Seismic Design of Buildings) emphasizes the pivotal role of load combinations in structural analyses and offers a calculated method to determine the appropriate combinations of loads as below:

$$LC = 1.0 \cdot DL + 0.5 \cdot LL \tag{3}$$

where $LC$ is load combinations, $DL$ and $LL$ are Dead Load and Live Load separately.

The nonlinear pushover analysis is designed to use a displacement control system, where control is maintained through conjugate displacement. The analysis is structured to include 50 steps, each systematically accounting for different displacements. This comprehensive range of data points allows for a detailed exploration of the structure's response to progressively increasing lateral loads. By varying the displacement levels, the analysis thoroughly examines the behavior of the structure, capturing the evolution of deformations and identifying critical points in the load-displacement relationship. This 50-step design is expected to ensure a meticulous and thorough assessment of the structure's performance under seismic conditions.

## 3. Discussion of Nonlinear Pushover Analysis

### 3.1. Performance Point

The analysis includes results presented in Tables 5-6, providing a comprehensive overview of the performance points for CASE-1 to CASE-5. These performance points are assessed under the guidelines of ACT-40 and FEMA 440, which inform the evaluation of structural performance under seismic conditions. By following these guidelines, the analysis ensures a detailed and accurate assessment of how the structure responds to seismic forces. This thorough presentation of results across different cases enables an understanding of the structural behavior and performance under varying RC footing in this research.

For the external elevator project located on Jinzhong Rd in Shanghai City, the

performance points of the external elevator well are defined according to Tables 5.1.4-1 and 5.1.4-2 of the Chinese standard GB 50011-2010 (Code for Seismic Design of Buildings). The seismic intensity in this area is classified as 7, with a seismic acceleration of 0.1 g. Additionally, the maximum influence factor is set at 0.12, the characteristic ground period is determined to be 0.4, and the period time discount factor is 1. These parameters ensure that the structural performance evaluation aligns with the specific seismic conditions and requirements of the project location, providing a thorough and accurate assessment of the seismic resilience of the external elevator well in this research.

Referring to the results of the performance point under ACT-40, as illustrated in Table 5, it is evident that the height of the RC footing significantly influences the structural performance. Specifically, increasing the height of the RC footing decreases both the base shear and the structural lateral displacement. In terms of $S_a$ (Spectral acceleration) and $S_d$ (Spectral displacement), the results indicate that a higher footing height leads to an increase in $S_a$ but a decrease in $S_d$. Furthermore, the structural period, a critical evaluation criterion for seismic performance, also decreases as the height of the RC footing increases. These findings highlight the pivotal role of the RC footing height in enhancing the overall seismic resilience of the structure.

Similar to the results in Table 5, the results of the performance point under FEMA 440, as illustrated in Table 6, also confirm that the height of the RC footing significantly influences structural performance, specifically, increasing the height of the RC footing results in a decrease in both the base shear and the structural lateral displacement. Additionally, a higher footing height leads to an increase in $S_a$ and a decrease in $S_d$. Furthermore, the structural period also decreases as the height of the RC footing increases.

**Table 5.** Performance point under ACT-40.

| Types | Base Shear | Displacement | Sa | Sd | Teff |
|---|---|---|---|---|---|
| | kN | mm | g | mm | sec |
| CASE-1 | 48.944 | 82.356 | 1.131 | 53.686 | 0.437 |
| CASE-2 | 48.731 | 79.105 | 1.156 | 51.475 | 0.423 |
| CASE-3 | 48.414 | 75.792 | 1.181 | 49.277 | 0.413 |
| CASE-4 | 47.814 | 72.295 | 1.199 | 47.012 | 0.397 |
| CASE-5 | 46.557 | 68.131 | 1.199 | 44.342 | 0.386 |

**Table 6.** Performance point under FEMA 440.

| Types | Base Shear | Displacement | Sa | Sd | Teff |
|---|---|---|---|---|---|
| | kN | mm | g | mm | sec |
| CASE-1 | 48.945 | 82.358 | 1.131 | 53.688 | 0.437 |
| CASE-2 | 48.733 | 79.108 | 1.157 | 51.477 | 0.423 |
| CASE-3 | 48.417 | 75.798 | 1.181 | 49.281 | 0.411 |
| CASE-4 | 47.821 | 72.305 | 1.199 | 47.016 | 0.397 |
| CASE-5 | 46.566 | 68.143 | 1.199 | 44.352 | 0.386 |

### 3.2. Capacity Curve

The evaluation of structural performance under nonlinear pushover analysis relies significantly on the results derived from the capacity curve. This curve is a fundamental component in understanding how the structure responds to incremental lateral loads, offering valuable insights into its overall seismic performance. The capacity curve identifies critical points where the structure may experience significant deformations or failures. Figure 5 provides a visual representation of the capacity curves for each specific external elevator well structure in this research, illustrating how the different height of the RC footing responds to seismic forces.

Referring to the results of the capacity curves in Figure 5, it is evident that increasing the height of the RC footing raises the base shear value for the entire structure of the external elevator well. Additionally, the results of the capacity curves also show that lower heights of the RC footing result in longer lateral displacements for the same base shear value. Furthermore, based on the results of capacity curves, Table 7 shows that the height of the RC footing influences the slope of the elastic zone. As the height increases, so does the slope value in the elastic zone under nonlinear pushover analysis. Notably, the most significant increase occurs between CASE-3 and CASE-4, representing footing heights of 900 mm to 1200 mm, while a lower increase ratio is observed between CASE-4 and CASE-5, representing heights of 1200 mm to 1500 mm. These findings highlight the critical role of RC footing height in enhancing the structural performance and stability of the external elevator well under seismic conditions.

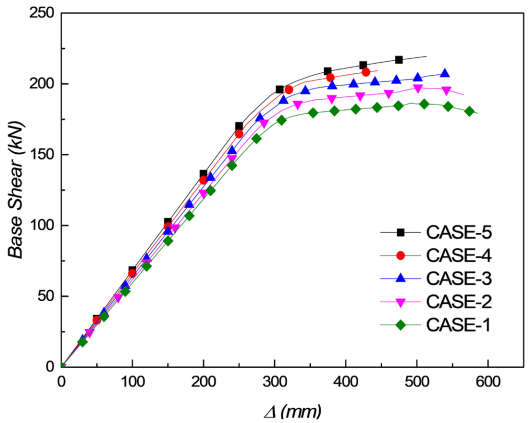


Figure 5. Capacity curves.

Table 7. Slope of the elastic zone.

| Types | Slope | Ratio |
|---|---|---|
| CASE-1 | 0.5936 | 0.00% |
| CASE-2 | 0.6148 | 3.57% |
| CASE-3 | 0.6373 | 3.66% |
| CASE-4 | 0.6631 | 4.05% |
| CASE-5 | 0.6822 | 2.88% |

### 3.3. Capacity Spectrum

In evaluating the seismic performance of a building, the capacity spectrum method is instrumental in determining the building's performance level. This method involves establishing a target displacement and conducting a graphical comparison between the structure's capacity and the seismic demand. A key feature of the capacity spectrum method is its ability to visually represent the structure's capacity and response to seismic forces.

Referring to Riza Ainul Hakim *et al.* [10], the process of converting the capacity curve to the capacity spectrum involves calculating the modal participation factor ( $MPF_1$ ) and the modal mass coefficient ( $a$ ) through the specific equations below:

$$MPF_1 = \frac{\sum m_i \phi_{i1}}{\sum m_i \phi_{i1}^2} \tag{4}$$

$$a = \frac{\left[\sum m_i \phi_{i1}\right]^2}{\left[\sum_{i=1}^{N} \frac{w_i}{g}\right] \cdot \left[\sum_{i=1}^{N} m_i \phi_{i1}^2\right]} \tag{5}$$

where $\frac{w_i}{g}$ is mass assigned to level $i$, $\phi_{i1}$ is the amplitude of model 1 at level $i$, and $N$ is level $N$.

Based on the values of $MPF_1$ and $a$ are calculated, the values of $S_a$ (spectral acceleration) and $S_d$ (spectral displacement) are computed for each point along the capacity curve using the equations below:

$$\frac{S_a}{g} = \frac{V_b}{w} \cdot \frac{1}{a} \tag{6}$$

$$S_d = \frac{\Delta_{roof}}{MPF_1 \cdot \phi_{roof_1}} \tag{7}$$

where $V_b$ is base shear force, $w$ is building load weight, and $\Delta_{roof}$ is roof displacement.

To transform a demand spectrum from $S_a$ (spectral acceleration) and $T$ (period) format to *ADRS* (Acceleration Displacement Response Spectrum) format, it is necessary to compute the value of $S_d$ (spectral displacement) for each point on the curve using the equation below:

$$S_d = \frac{T^2 S_a}{4\pi^2} \tag{8}$$

The performance point is determined by overlaying the demand spectrum onto the capacity curve in spectral coordinates or ADRS format, and this process is facilitated by the built-in capacity spectrum method within the SAP 2000.

Referring to **Figure 6**, the specific response spectrum of GB 50011-2010 (Code for Seismic Design of Buildings) is provided for evaluating the performance points of the external elevator project for an existing RC building in Jinzhong Rd, Shanghai City (121˚36'69"E, 31˚21'99"N). The results indicate that all five

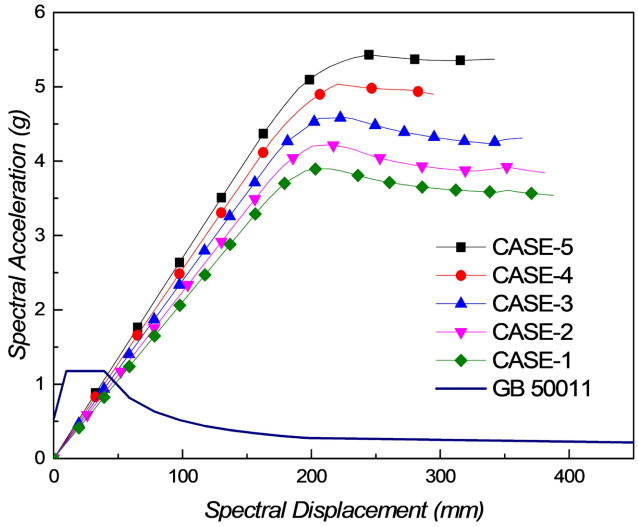


**Figure 6.** Capacity spectrum.

different designs of the external elevator satisfy the GB 50011-2010 code. However, a comparison of the five different capacity spectrums reveals that the height of the RC footing significantly influences the overall structure of the external elevator well. Higher RC footings result in faster $S_a$ (Spectrum acceleration) and shorter $S_d$ (Spectrum displacement). This analysis underscores the critical influence of footing height on the seismic performance and stability of the external elevator structure, aligning with the findings from the capacity curve.

### 3.4. Layer Displacement and Drift Ratio

The states of plastic hinges are crucial in evaluating the performance of structures under nonlinear pushover analysis. The research of Van Long Hoang *et al.* [19] emphasizes the importance of analyzing plastic hinge states in steel frames under static loads, highlighting how the plastic hinge states influence structural performance. Furthermore, the research of Yi Zhou *et al.* [20] underscores the significance of plastic hinge analysis in welded high-strength steel frames, analyzing various steel frame designs through the plastic hinge states. Both studies demonstrate that understanding the behavior of plastic hinges is essential for assessing the resilience and integrity of steel frame structures under different loading conditions.

According to the code of ASCE 41 - 13, which is used for plastic hinge analysis in SAP 2000, the different stages of plastic hinge formation are illustrated in Figure 7. The linear response occurs between point A (unloaded element) and the effective yield point B. The slope from point B to point C is typically a small percentage (0% to 10%) of the elastic slope, representing phenomena such as strain hardening. Point C represents the strength of the element, with an abscissa value indicating the deformation where significant strength degradation begins, leading from point C to point D. Beyond point D, the element's strength substantially reduces until point E, where the seismic strength is essentially zero.

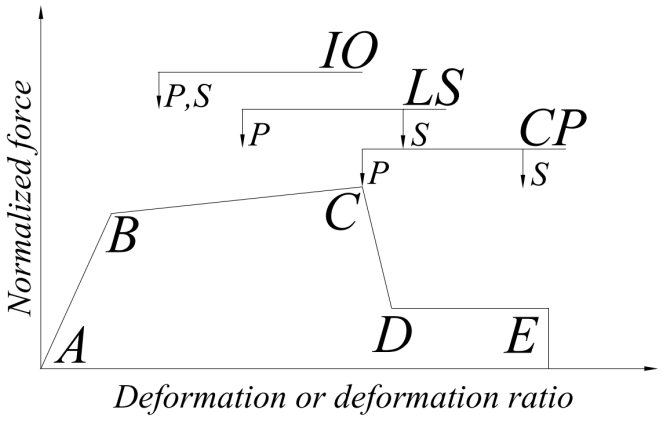


**Figure 7.** Capacity spectrum.

In the plastic range, acceptance criteria for deformation or deformation ratios for P (Primary components) and S (Secondary components) are defined corresponding to the target structure performance levels: IO (Immediate Occupancy), LS (Life Safety), and CP (Collapse Prevention), as shown in **Figure 7**. Referring to Mircea D. Botez *et al.* [21], IO indicates a structural performance level where only very limited structural damage has occurred, allowing the building to remain usable post-earthquake. LS represents a performance level where significant damage has occurred, but there is still some margin against partial or total structural collapse, ensuring occupant safety. CP signifies a performance level where the building is on the verge of partial or total collapse, indicating a severe damage state.

Previous research emphasizes that layer displacement and layer drift ratio are critical analytical results for evaluating structural seismic behavior [22]-[25]. In line with the characteristics of nonlinear pushover analysis, this research examines these metrics for the external elevator structure. Referring to **Figures 8-12**, the analysis is conducted under plastic hinge conditions at the effective yield point B and the collapse prevention point CP. This approach provides a comprehensive understanding of how the external elevator structure responds to seismic forces, offering insights into its performance at different stages of deformation.

Referring to **Figures 8-12**, the structural displacement at plastic hinge B (Effective Yield) point increases as the height of the RC footing increases, a trend also evident in graph (a) of **Figure 13**. Additionally, when plastic hinges are at the CP (Collapse Prevention) point, despite some inconsistent displacement results in CASE-3, the results still show that higher RC footings generally lead to longer displacements, as depicted in graph (b) of **Figure 13**. However, the analysis also reveals that lower heights of the RC footing cause significant damage to the column section on the first floor. This is indicated by the increased number of plastic hinges appearing at the bottom of the entire external elevator structure. Moreover, this phenomenon is further discussed in the layer drift ratio results, as illustrated in both graphs of **Figure 14**.

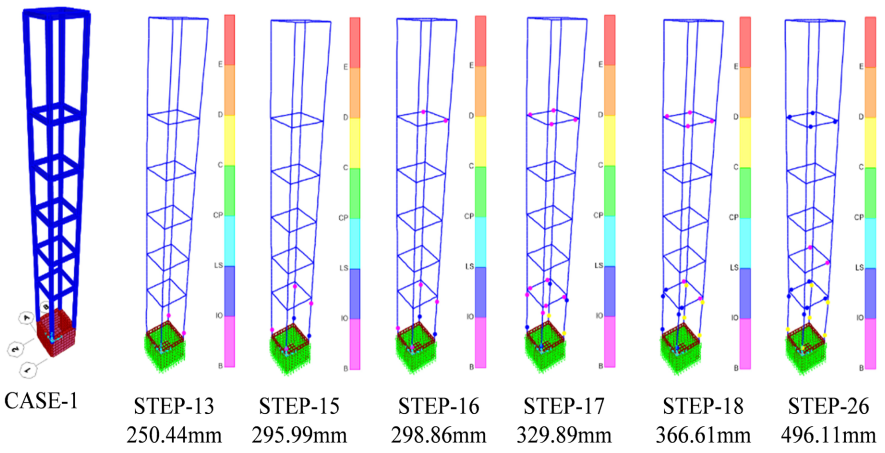


B: STEP-13 (250.44 mm); CP: STEP-17 (329.89 mm)

**Figure 8.** Development and distribution of plastic hinges (CASE-1).

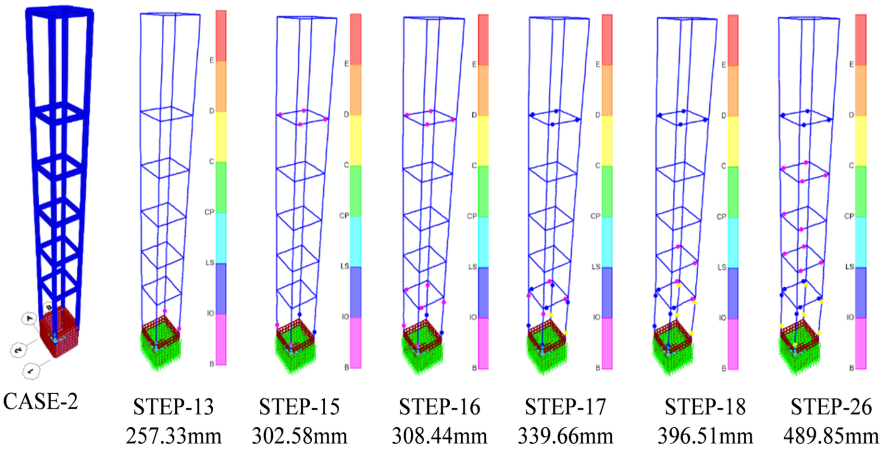


B: STEP-13 (257.33 mm); CP: STEP-17 (339.66 mm)

**Figure 9.** Development and distribution of plastic hinges (CASE-2).

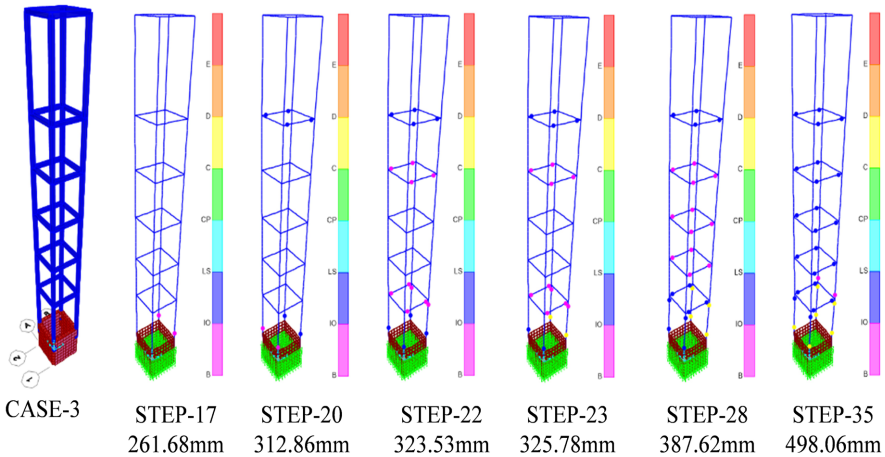


B: STEP-17 (261.68 mm); CP: STEP-23 (325.78 mm)

**Figure 10.** Development and distribution of plastic hinges (CASE-3).

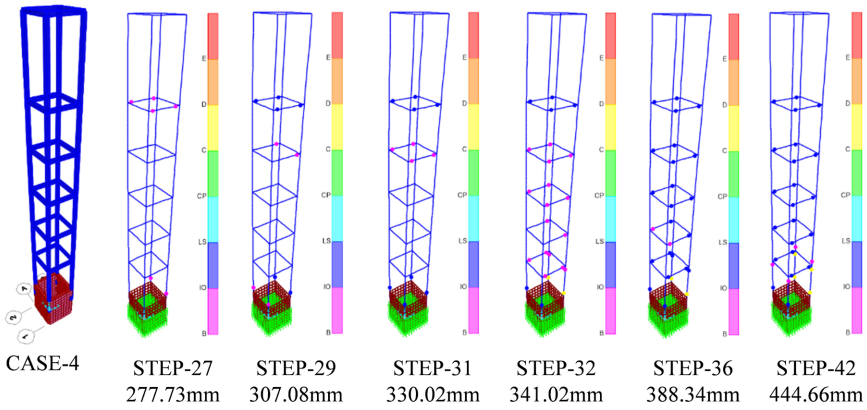


B: STEP-27 (277.73 mm); CP: STEP-32 (341.02 mm)

**Figure 11.** Development and distribution of plastic hinges (CASE-4).

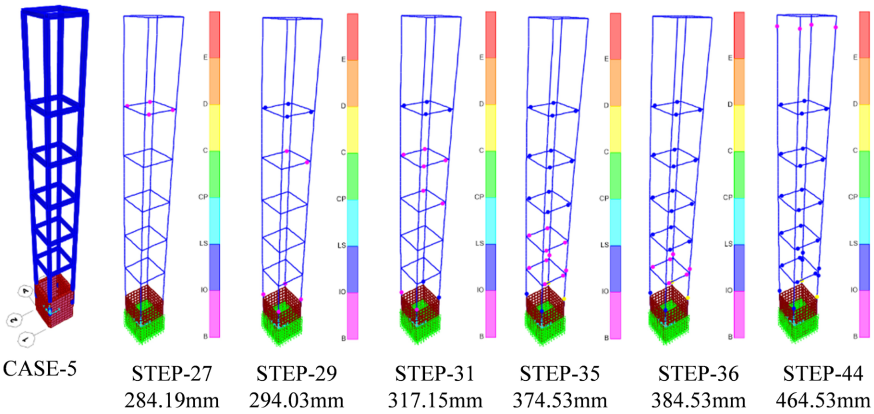


B: STEP-27 (284.19 mm); CP: STEP-35 (374.53 mm)

**Figure 12.** Development and distribution of plastic hinges (CASE-5).

Based on the results of layer displacement, the findings indicate that higher RC footings lead to longer overall structural lateral displacement, as illustrated in graph (a) of **Figure 13**. However, when examining the lower floors of the external elevator well, longer lateral displacements occur with lower RC footings. This trend is less clear when plastic hinges reach the CP (Collapse Prevention) point compared to the B (Effective Yield) point. Nonetheless, higher RC footings consistently result in longer overall displacement, while lower floors experience greater displacement with lower RC footings, as depicted in graph (b) of **Figure 13**. These findings highlight the complex impact of footing height on structural lateral displacement across different floors of the external elevator well during seismic events.

The layer drift ratio for each distinct story in the external elevator well is determined by calculating the ratio of the structural lateral displacement to the story height. This involves using the equations to accurately assess how much each story displaces laterally relative to its height as below:

$$\Delta = \delta_x - \delta_{x-1} \tag{9}$$

$$\Delta_{ratio} = \frac{\Delta}{h} \tag{10}$$

where $\delta_x$ is the displacement at the $x$ floor, $\delta_{x-1}$ is the displacement at the $x-1$ floor, $\Delta$ is the drift between the $x$ floor and the $x-1$ floor, $h$ is the height of the story, and $\Delta_{ratio}$ is the drift ratio.

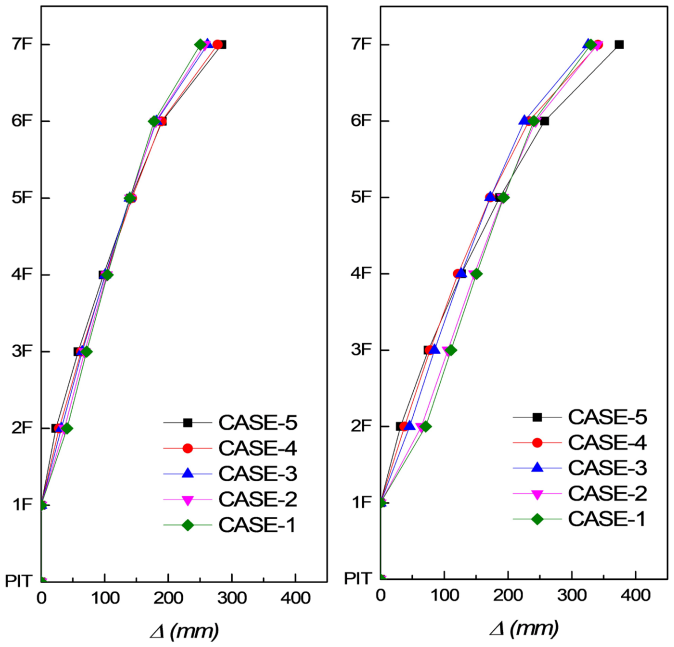


(a) Plastic hinge on B state (b) Plastic hinge on CP state

**Figure 13.** Layer displacement.

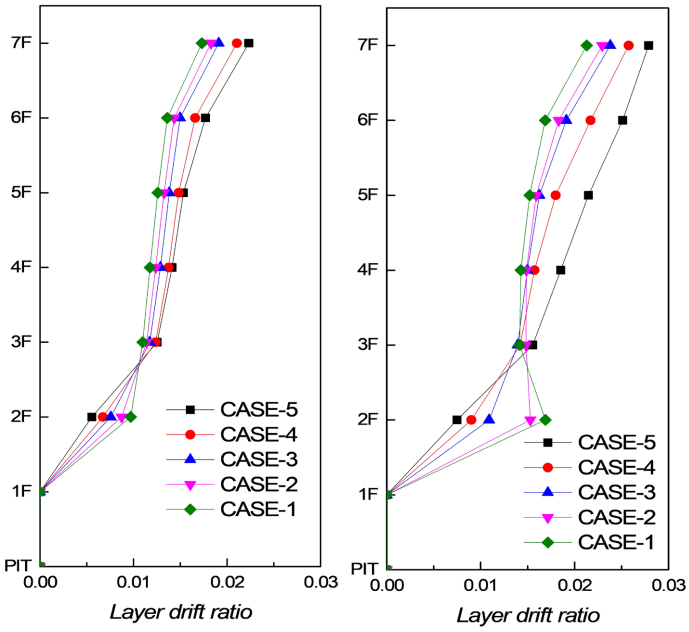


(a) Plastic hinge on B state (b) Plastic hinge on CP state

**Figure 14.** Layer drift ratio.

Based on the results of layer displacement in Figure 13, the layer drift ratio can be calculated through equations (9) and (10), with the results illustrated in Figure 14. The findings emphasize that higher RC footings in the external elevator well lead to larger overall layer drift ratios. However, when focusing on the lower floors, larger drift ratios occur with lower RC footings. These trends are observed at both the B (Effective Yield) and CP (Collapse Prevention) points, as shown in graphs (a) and (b) of Figure 14, highlighting the influences of the RC footing height on the drift ratio across different stories of the structure.

The discussion delves into how the height of RC footings influences the performance of the external elevator structure as a whole. It underscores that higher RC footings enhance the ability of the structure to withstand seismic forces, resulting in improved performance during nonlinear pushover analysis. Essentially, higher RC footings enhance the resistance of the structure to seismic events, indicating a more robust design.

Moreover, due to the taller first-floor height (4200 mm) than other floors (2800 mm), the taller first-floor height reveals a mechanical separation effect due to the longer columns. This mechanical separation effect has a detrimental impact on overall structural performance during nonlinear pushover analysis. However, the research findings indicate that higher RC footings counteract this effect. By avoiding the stress concentration on first-floor columns, higher footings mitigate the mechanical separation due to the long column, leading to enhanced overall structural performance.

## 4. Conclusions

As the number of external elevator installations in existing RC buildings increases, these projects are recognized for contributing to sustainable development by reducing carbon dioxide emissions. However, the seismic performance of external elevators has not been extensively studied. To address this gap and provide valuable insights, this research investigates the effect of the height of RC footings on the structural performance of external elevators. Using an actual external elevator project on Jinzhong Road in Shanghai City, this research explores how varying RC footing heights influence the structural ability to withstand seismic events, thereby enriching the reference material available for future external elevator projects and enhancing the design for better performance under seismic conditions.

The analysis of performance points revealed that higher RC footings result in smaller base shear and shorter displacement. Although higher footings might show a reduction in base shear, they offer the significant advantage of reduced displacement. Shorter displacement helps in minimizing structural deformation, thus preventing damage during seismic events. The results for $S_a$ (Spectral acceleration) and $S_d$ (Spectral displacement) corroborate these findings, indicating that higher RC footings enhance the overall seismic performance of the structure. Furthermore, structures with shorter periods generally experience less am-

plification of seismic forces, remain stiffer, and undergo less deformation. Consequently, the performance points analysis also highlighted the benefits of higher RC footings, demonstrating the effectiveness in improving the seismic resilience of external elevator wells.

The analysis of the capacity curve and capacity spectrum revealed that higher RC footings improve structural performance under seismic conditions. Specifically, higher RC footings were associated with increased base shear and faster $S_a$ (Spectrum acceleration) throughout the nonlinear pushover analysis. At the same time, the higher RC footings led to a decrease in displacement and $S_d$ (Spectrum displacement). These findings provide clear evidence that higher RC footings can significantly enhance the seismic resilience of a structure, effectively reducing deformation and potential damage during an earthquake. The increased base shear capacity and reduced displacement highlight the improved stability and stiffness of the structure, affirming the advantages of higher RC footings in external elevator wells.

The findings on layer displacement and layer drift ratio under the plastic hinge state underscore the benefits of higher RC footings for external elevator wells, specifically, increased footing height enhances seismic performance, reducing structural deformation. However, prior research suggests that higher RC infills may induce short-column effects [26]-[30], which can influence structural performance during seismic events. Therefore, while this research serves as a valuable reference for external elevator projects, it also indicates the necessity of further investigation into the short-column effect caused by higher RC footings.

## Acknowledgements

The research described in this paper was financially supported by Shanghai HaXell elevator and performed at Kyungpook National University.

## Conflicts of Interest

The authors declare no conflicts of interest regarding the publication of this paper.

## References

[1] Tan, Y., Liu, G., Zhang, Y., Shuai, C. and Shen, G.Q. (2018) Green Retrofit of Aged Residential Buildings in Hong Kong: A Preliminary Study. *Building and Environment*, **143**, 89-98. https://doi.org/10.1016/j.buildenv.2018.06.058

[2] Pheng Low, S., Gao, S. and Lin Tay, W. (2014) Comparative Study of Project Management and Critical Success Factors of Greening New and Existing Buildings in Singapore. *Structural Survey*, **32**, 413-433. https://doi.org/10.1108/ss-12-2013-0040

[3] Shi, M., Sun, E., Xu, X. and Choi, Y. (2024) Prediction and Analysis of Elevator Traffic Flow under the LSTM Neural Network. *Intelligent Control and Automation*, **15**, 63-82. https://doi.org/10.4236/ica.2024.152004

[4] Niedostatkiewicz, M., Majewski, T. and Ziółkowski, P. (2019) Design Errors of the External Lift Shaft and Their Negative Impact on the Operation of the Clinic Build-

ing. *MATEC Web of Conferences*, **284**, Article No. 02006. https://doi.org/10.1051/matecconf/201928402006

[5] Dai, X., Li, Z., Ma, L. and Jin, J. (2022) The Spatio-Temporal Pattern and Spatial Effect of Installation of Lifts in Old Residential Buildings: Evidence from Hangzhou in China. *Land*, **11**, Article No. 1600. https://doi.org/10.3390/land11091600

[6] Yusra, A., Mustafa, A., Refiyanni, M. and Zakia, Z. (2023) Performance Structural Analysis of U2C Building with the Kobe Earthquake Spectrum. *International Journal of Engineering, Science and Information Technology*, **3**, 36-46. https://doi.org/10.52088/ijesty.v3i1.413

[7] Nguyen, V., Nizamani, Z.A., Park, D. and Kwon, O. (2020) Numerical Simulation of Damage Evolution of Daikai Station during the 1995 Kobe Earthquake. *Engineering Structures*, **206**, Article ID: 110180. https://doi.org/10.1016/j.engstruct.2020.110180

[8] Hökelekli, E., Demir, A., Ercan, E., Nohutçu, H. and Karabulut, A. (2020) Seismic Assessment in a Historical Masonry Minaret by Linear and Non-Linear Seismic Analyses. *Periodica Polytechnica Civil Engineering*, **4**, 438-448. https://doi.org/10.3311/ppci.15126

[9] Jan, T.S., Liu, M.W. and Kao, Y.C. (2004) An Upper-Bound Pushover Analysis Procedure for Estimating the Seismic Demands of High-Rise Buildings. *Engineering Structures*, **26**, 117-128. https://doi.org/10.1016/j.engstruct.2003.09.003

[10] Hakim, R.A., Alama, M.S.A. and Ashour, S.A. (2014) Seismic Assessment of an RC Building Using Pushover Analysis. *Engineering, Technology & Applied Science Research*, **4**, 631-635. https://doi.org/10.48084/etasr.428

[11] Mohod, M.V. (2015) Pushover Analysis of Structures with Plan Irregularity. *IOSR Journal of Mechanical and Civil Engineering*, **12**, 46-55.

[12] Ruggieri, S. and Uva, G. (2020) Accounting for the Spatial Variability of Seismic Motion in the Pushover Analysis of Regular and Irregular RC Buildings in the New Italian Building Code. *Buildings*, **10**, Article No. 177. https://doi.org/10.3390/buildings10100177

[13] Habibi, A., Saffari, H. and Izadpanah, M. (2019) Optimal Lateral Load Pattern for Pushover Analysis of Building Structures. *Steel and Composite Structures*, **32**, 67-77.

[14] Shehu, R. (2021) Implementation of Pushover Analysis for Seismic Assessment of Masonry Towers: Issues and Practical Recommendations. *Buildings*, **11**, Article No. 71. https://doi.org/10.3390/buildings11020071

[15] Yacila, J., Camata, G., Salsavilca, J. and Tarque, N. (2019) Pushover Analysis of Confined Masonry Walls Using a 3D Macro-Modelling Approach. *Engineering Structures*, **201**, Article ID: 109731. https://doi.org/10.1016/j.engstruct.2019.109731

[16] Bhandari, M., Bharti, S.D., Shrimali, M.K. and Datta, T.K. (2018) Assessment of Proposed Lateral Load Patterns in Pushover Analysis for Base-Isolated Frames. *Engineering Structures*, **175**, 531-548. https://doi.org/10.1016/j.engstruct.2018.08.080

[17] Ismaeil, M., Sobaih, M. and Akl, A. (2015) Seismic Capacity Assessment of Existing RC Buildings in the Sudan by Using Pushover Analysis. *Open Journal of Civil Engineering*, **5**, 154-174. https://doi.org/10.4236/ojce.2015.52016

[18] Alkhamis, M.T. and AL-Rashidi, A. (2023) Finite Element Analysis of the Influence of Artificial Cementation on the Strength Parameters and Bearing Capacity of Sandy Soil under a Strip Footing. *Open Journal of Civil Engineering*, **13**, 221-236. https://doi.org/10.4236/ojce.2023.132017

[19] Hoang, V., Nguyen Dang, H., Jaspart, J. and Demonceau, J. (2015) An Overview of the Plastic-Hinge Analysis of 3D Steel Frames. *Asia Pacific Journal on Computational Engineering*, **2**, Article No. 4. https://doi.org/10.1186/s40540-015-0016-9

[20] Zhou, Y., Huang, D., Li, T. and Li, Y. (2022) Second-Order Arbitrarily-Located-Refined Plastic Hinge Model for High-Strength Steel Frame Design. *Journal of Constructional Steel Research*, **190**, Article ID: 107112. https://doi.org/10.1016/j.jcsr.2021.107112

[21] Botez, M.D., Bredean, L.A. and Ioani, A.M. (2014) Plastic Hinge vs. Distributed Plasticity in the Progressive Collapse Analysis. *Acta Technica Napocensis*: *Civil Engineering & Architecture*, **57**, 24-36.

[22] Liu, C., Sun, P. and Shi, R. (2020) Seismic Response Analysis and Control of Frame Structures with Soft First Storey under Near-Fault Ground Motions. *Advances in Civil Engineering*, **2020**, Article ID: 2642431. https://doi.org/10.1155/2020/2642431

[23] Abdulsadah Mohammed, H. and Shawky Abdulsahib, W. (2024) Investigation of Seismic Response of Irregular Steel Buildings: A Case Study of U-Shaped Structures. *BIO Web of Conferences*, **97**, Article No. 00079. https://doi.org/10.1051/bioconf/20249700079

[24] Chao, S., Karki, N.B. and Sahoo, D.R. (2013) Seismic Behavior of Steel Buildings with Hybrid Braced Frames. *Journal of Structural Engineering*, **139**, 1019-1032. https://doi.org/10.1061/(asce)st.1943-541x.0000702

[25] Peng, Z., Guo, Z., Shen, Y. and Wang, X. (2023) Inter-Story Drift Ratio Detection of High-Rise Buildings Based on Ambient Noise Recordings. *Applied Sciences*, **13**, Article No. 6724. https://doi.org/10.3390/app13116724

[26] Shi, M., Choi, Y. and Kang, S. (2023) A Study of the Infill Wall of the RC Frame Using a Quasi-Static Pushover Analysis. *Computers and Concrete*, **32**, 455-464.

[27] Cagatay, I.H., Beklen, C. and Mosalam, K.M. (2010) Investigation of Short Column Effect of RC Buildings: Failure and Prevention. *Computers & Concrete*, **7**, 523-532. https://doi.org/10.12989/cac.2010.7.6.523

[28] Shi, M., Xu, X. and Choi, Y. (2023) Study on the RC Frame with the Partial Infill Wall in Pushover Analysis. *Scientific Journal of Technology*, **5**, 13-22. https://doi.org/10.54691/sjt.v5i9.5586

[29] Kaish, A.B.M.A., Alam, M.R., Jamil, M., Zain, M.F.M. and Wahed, M.A. (2012) Improved Ferrocement Jacketing for Restrengthening of Square RC Short Column. *Construction and Building Materials*, **36**, 228-237. https://doi.org/10.1016/j.conbuildmat.2012.04.083

[30] Guevara, L.T. and García, L.E. (2005) The Captive- and Short-Column Effects. *Earthquake Spectra*, **21**, 141-160. https://doi.org/10.1193/1.1856533